were cytodifferentiated for 1 week in the presence of M-CSF (macrophage colony stimulating factor) and RANKL (receptor activator of NFκB ligand) (Koga et al., 2004). TRAP-positive osteoclasts emerged after 3 days of culture (Figure 1E). The number of TRAP-positive osteoclasts and the number of LacZ-expressing cells simultaneously increased. In the contrast, the LacZ expression was not detected in primary cultured osteoblasts derived from the calvaria (Figure S1F). In view of both our in vivo and in vitro observations, we conclude that the $Ctsk^{Cre/+}$ mouse line expresses Cre in differentiated osteoclasts. Moreover, estrogen response in bone mass control was not distinguishable in between $Ctsk^{Cre/+}$ and $Ctsk^{+/+}$ mice (Figure S2A).

We then crossed floxed *ERα* mice (Dupont et al., 2000) with $Ctsk^{Cre/+}$ mice to disrupt ERα in differentiated osteoclasts ($ER\alpha^{\Delta Oc/\Delta Oc}$). Excision of the *ERα* gene (Figure S1G) was confirmed by Southern blotting of DNA from adult female and male (data not shown) bone as well as in cultured mature osteoclasts (Figure S1H). No overt differences were observed in the growth curve, reproduction, or tissues for up to 12 weeks of age (Figure 1F) between the $Ctsk^{Cre/+}$; $ER\alpha^{+/+}$ ($ER\alpha^{+/+}$) and the $Ctsk^{Cre/+}$; $ER\alpha^{flox/flox}$ ($ER\alpha^{\Delta Oc/\Delta Oc}$) mice, with the exception of the female bones. Serum levels of sex hormones and bone remodeling regulators such as IGF-I, leptin, and follicle-stimulating hormone (Sun et al., 2006; Takeda et al., 2002) appeared unchanged in both male and female $ER\alpha^{\Delta Oc/\Delta Oc}$ mice at 12 weeks (Figure 1G).

Osteopenia Occurred in Osteoclast-Specific ERα KO Females But Not Males

The 12-week-old $ER\alpha^{\Delta Oc/\Delta Oc}$ females exhibited a clear reduction in bone mineral density (BMD) in the femurs (Figures 2A–2C) and tibiae (data not shown) when compared with $ER\alpha^{+/+}$ mice. Though cortical bone appeared unaffected, trabecular bone loss (Figure 2A) with significant reduction of trabecular bone volume (BV/TV) (Figure 2F) was clearly seen. This is similar to the osteoporotic abnormalities observed in women during natural menopause or following ovariectomy (Delmas, 2002; Tolar et al., 2004). However, unlike men deficient in aromatase or ERα activity (Simpson and Davis, 2001; Smith et al., 1994), $ER\alpha^{\Delta Oc/\Delta Oc}$ males unexpectedly exhibited no clear bone loss even in the trabecular areas (Figures 2A–2C). In $ER\alpha^{\Delta Oc/\Delta Oc}$ females, both the bone-formation rate, estimated by double-calcein labeling (Figure 2D), as well as the bone-resorption rate, estimated from TRAP-positive differentiated osteoclast numbers (Figure 2E), were increased, indicating high bone turnover. Histomorphometric analyses of $ER\alpha^{\Delta Oc/\Delta Oc}$ females supported the observation of accelerated bone resorption, as increased numbers of osteoclasts (Oc. S/BS and N. Oc/BS) were observed together with more eroded bone surface (ES/BS in Figure 2F). Bone formation was also enhanced as the rates of mineral apposition (MAR) and bone formation (BFR/BS) were both upregulated without an increase in osteoblast numbers (Ob.S/BS) (Figure 2F). Thus, considering all of these findings, it is conceivable that the increased number of differentiated osteoclasts following ERα ablation accelerates bone resorption over formation, leading to bone loss in the trabecular areas.

No Further Bone Loss Results from Estrogen Deficiency in $ER\alpha^{\Delta Oc/\Delta Oc}$ Females

To verify whether osteoclastic ERα indeed mediates osteoprotective estrogen actions, estrogen action was investigated by ovariectomy (OVX) of 12-week-old female mice. As expected, OVX in $ER\alpha^{+/+}$ females resulted in significantly reduced BMD particularly in the trabecular bone (Figures 3A and 3B) but not in the cortical bone (Figure 3C). Consistent with previous reports, (Kimble et al., 1995; Teitelbaum and Ross, 2003), estrogen deficiency following OVX upregulated the serum levels of cytokines like TNFα and IL-1α (Figure 3D). These cytokines enhance bone resorption through stimulation of osteoclastogenesis, leading to the loss of bone mass (Teitelbaum and Ross, 2003). OVX did not further reduce BMD or trabecular bone volume of the femurs of $ER\alpha^{\Delta Oc/\Delta Oc}$ females (Figure 3B) nor affect increased number of TRAP-positive osteoclasts (see lower panel in Figure 3A) despite upregulation of serum cytokines. This suggests that the expression of cytokines known to regulate bone resorption is not under the control of osteoclastic ERα.

Estrogen Treatment Failed to Rescue the Osteoporotic Bone Phenotype of $ER\alpha^{\Delta Oc/\Delta Oc}$ Mice

Estrogen treatment by estrogen pellet implantation (OVX + E2) for 2 weeks after OVX in $ER\alpha^{+/+}$ mice elicited a dramatic increase in bone mass in both the trabecular and cortical areas of the femurs (data not shown) and lumbar vertebral bodies (Figure 4A). Estrogen action during E2 treatment in female mutants ($ER\alpha^{\Delta Oc/\Delta Oc}$) was not as pronounced as in the $ER\alpha^{+/+}$ females (Figures 4A and 4B), and the increase in the trabecular portions of the distal femurs was slight (data not shown). Histomorphometric analysis of the lumbar vertebral bodies (Figure 4B) supported the idea that E2 treatment in the female mutants was not sufficient to suppress accelerated bone resorption. These in vivo findings in the $ER\alpha^{\Delta Oc/\Delta Oc}$ females suggest that in at least the trabecular areas of the long bones and lumbar vertebral bodies, the osteoprotective estrogen action is primarily mediated via osteoclastic ERα inhibiting bone resorption.

To further test this hypothesis, we investigated ERα protein expression in mature osteoclasts from trabecular bone. Few reports document osteoclastic expression of ERα protein and an estrogen response in both intact animals and in in vitro cultured osteoclasts (Bland, 2000). We therefore reasoned that ER expression ceases during differentiation into mature cells from primary cultures of osteoclast precursors, similar to that observed in other primary culture cell systems such as avian oviduct cells, in which ERα protein expression is drastically decreased during culture (Kato et al., 1989). Using highly sensitive immunohistochemistry, we investigated whether

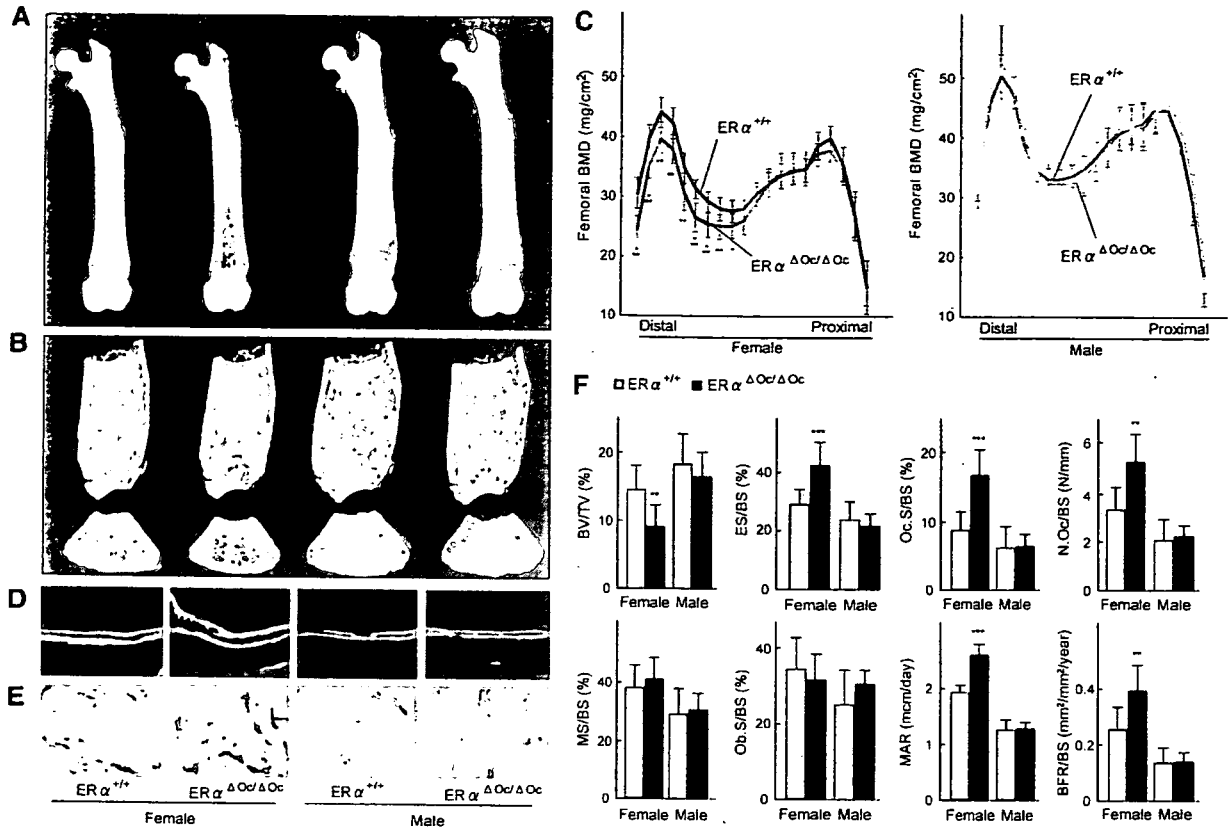

Figure 2. High Bone Turnover Osteopenia Was Observed in $ER\alpha^{\Delta Oc/\Delta Oc}$ Females But Not Males

(A) Soft X-ray images of femurs from 12-week-old $Ctsk^{Cre/+}$; $ER\alpha^{flox/flox}$ ($ER\alpha^{\Delta Oc/\Delta Oc}$) mice.

(B) Three-dimensional computed tomography images of the distal femurs and axial sections of distal metaphysis from representative 12-week-old $Ctsk^{Cre/+}$; $ER\alpha^{+/+}$ ($ER\alpha^{+/+}$) and $ER\alpha^{\Delta Oc/\Delta Oc}$ mice.

(C) BMD of each of 20 equal longitudinal divisions of femurs from 12-week-old $ER\alpha^{+/+}$ and $ER\alpha^{\Delta Oc/\Delta Oc}$ mice. (n = 10–11 animals per genotype; Student's t test, $^{*}p < 0.05$; $^{**}p < 0.01$; $^{***}p < 0.001$). Data are represented as mean ± SEM.

(D) Bone formation was also accelerated in $ER\alpha^{\Delta Oc/\Delta Oc}$ females when two calcein-labeled mineralized fronts visualized by fluorescent micrography were measured in the proximal tibia of 12-week-old mice.

(E) The number of TRAP-positive osteoclasts in the lumbar spine of female mice was increased by selective disruption of ERα in osteoclasts, indicating enhanced bone resorption.

(F) Bone turnover parameters as measured by dynamic bone histomorphometry after calcein labeling indicated high bone turnover in $ER\alpha^{\Delta Oc/\Delta Oc}$ females. Parameters are measured in the proximal tibia of 12-week-old $ER\alpha^{+/+}$ (open column) and $ER\alpha^{\Delta Oc/\Delta Oc}$ (filled column) mice. BV/TV: bone volume per tissue volume. ES/BS: eroded surface per bone surface. Oc.S/BS: osteoclast surface per bone surface. N.Oc/BS: osteoclast number per bone surface. MS/BS: mineralizing surface per bone surface. Ob.S/BS: osteoblast surface per bone surface. MAR: mineral apposition rate. BFR/BS: bone formation rate per bone surface (n = 10–11 animals per genotype; Student's t test, $^{*}p < 0.05$; $^{**}p < 0.01$; $^{***}p < 0.001$). Data are represented as mean ± SEM.

ERα protein expresses in differentiated osteoclasts in the bone tissues of femur sections from 12-week-old mice. ERα protein expression appeared abundant in osteoblasts and osteocytes of femur sections (Figure 4C) as well as hypothalamus (Figure S2B) from 12-week-old mice, in agreement with a previous report (Zaman et al., 2006). Likewise, expression levels of ERα in primary cultured osteoblasts derived from calvaria of $ER\alpha^{\Delta Oc/\Delta Oc}$ females appeared unaffected (Figure S2C). In contrast, in differentiated osteoclasts of the same femur sections, ERα expression was definitely detectable but very low in the $ER\alpha^{+/+}$ but undetectable in $ER\alpha^{\Delta Oc/\Delta Oc}$ females (Figure 4C).

Signaling by Osteoclastogenic Factors and Osteoclastogenesis Is Intact in Osteoclasts Deficient in ERα

It is possible that the osteoprotective function of osteoclastic ERα inhibits osteoclastogenesis. To address this issue, osteoclastogenesis was tested in cultured osteoclasts derived from bone-marrow cells of $ER\alpha^{\Delta Oc/\Delta Oc}$ mutants. In this cell culture system, a possible contribution of contaminated immune cells and stromal cells could be excluded, since osteoclastogenesis is only inducible by M-CSF treatment followed by M-CSF + RANKL (Koga et al., 2004).

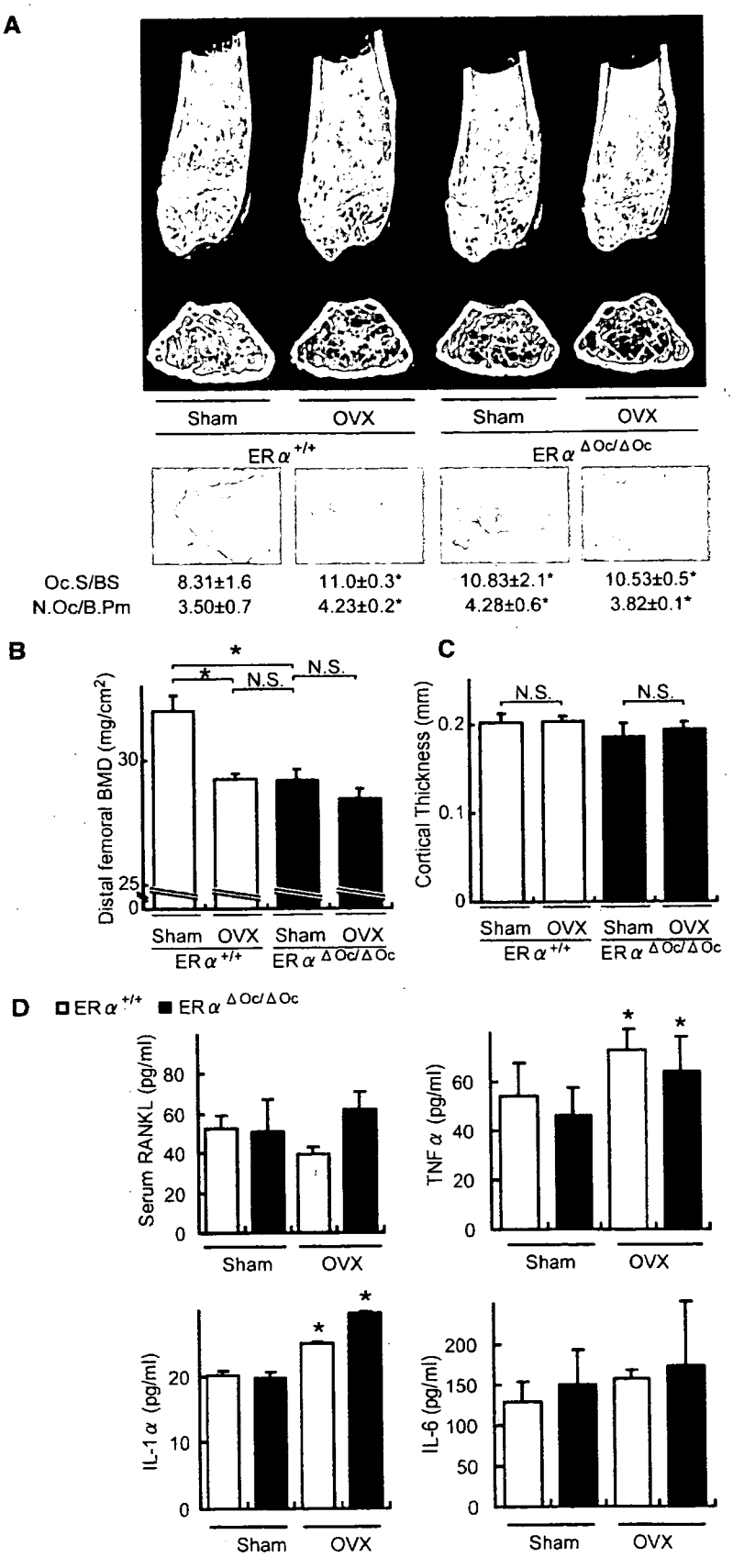

Figure 3. No Further Bone Loss of $ER\alpha^{\Delta Oc/\Delta Oc}$ Females by Ovariectomy

(A) Distal femoral micro CT analysis and lumbar vertebral bone histomorphometrical analysis of sham-operated or ovariectomized (OVX) 12-week-old $ER\alpha^{+/+}$ and $ER\alpha^{\Delta Oc/\Delta Oc}$ *mice* (*$p < 0.05$ compared to $ER\alpha^{+/+}$ sham group). Two weeks after OVX, the bone phenotype was analyzed.

(B) BMD of the distal femurs within each group are described in Figure 3A (*$p < 0.05$; N.S., not significant). Data are represented as mean ± SEM.

(C) Cortical thickness evaluation from micro CT analysis of femurs within each group described in Figure 3A. Data are represented as mean ± SEM.

(D) The levels of TNFα, IL-1α, and IL-6 in the bone-marrow cells culture media and serum RANKL (*$p < 0.05$ compared to each sham group). Data are represented as mean ± SEM.

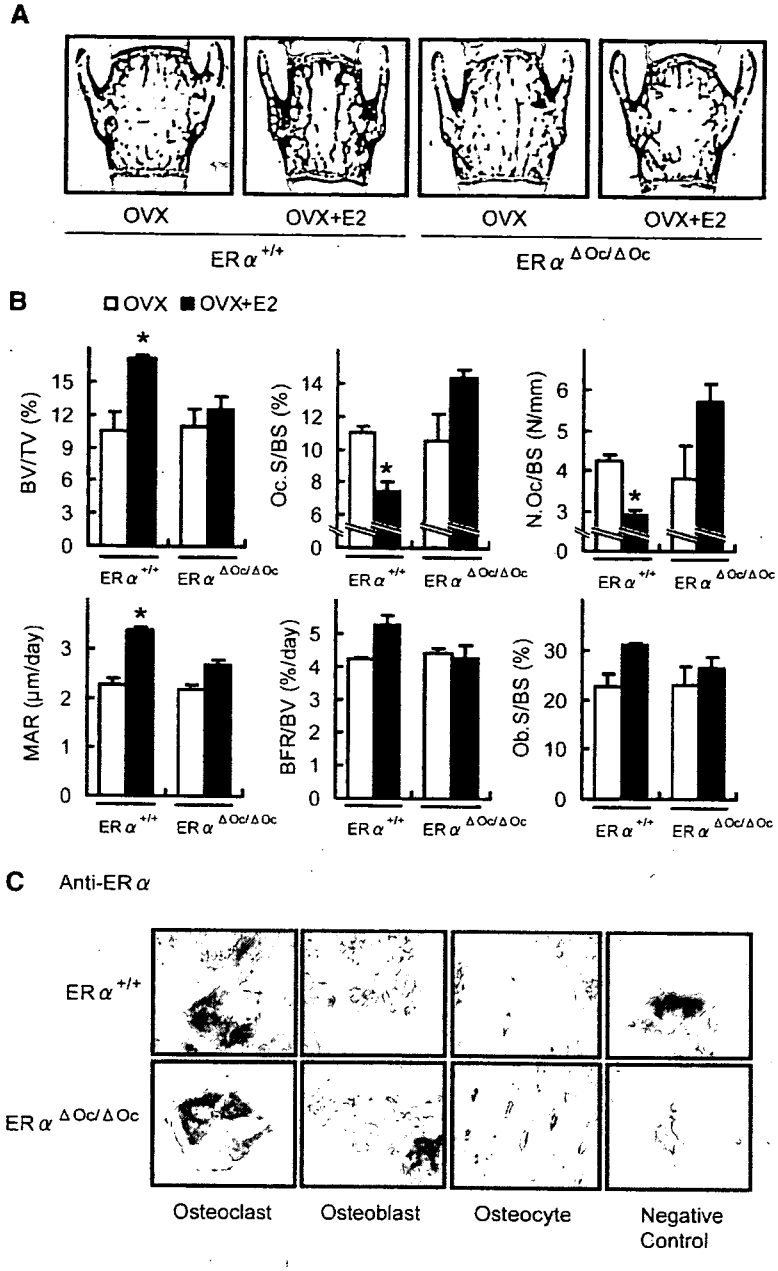

Figure 4. Estrogen treatment failed to reverse trabecular bone loss of ovariectomized $ER\alpha^{\Delta Oc/\Delta Oc}$ females

(A) von kossa staining of lumbar vertebral bodies of ovariectomized $ER\alpha^{+/+}$ and $ER\alpha^{\Delta Oc/\Delta Oc}$ mice treated with or without 17β-estradiol (0.83 μg/day) for 2 weeks (+E2) groups.

(B) Bone histomorphometrical analyses of the lumber vertebral bodies of 12-week-old ovariectomized $ER\alpha^{+/+}$ (left columns) and $ER\alpha^{\Delta Oc/\Delta Oc}$ (right columns) mice with (filled columns) or without (open columns) E2 treatment for 2 weeks (*$p < 0.05$ compared with E2-treated ovariectomized $ER\alpha^{\Delta Oc/\Delta Oc}$ mice). BV/TV: bone volume per tissue volume. ES/BS: eroded surface per bone surface. Oc.S/BS: osteoclast surface per bone surface. N.Oc/BS: osteoclast number per bone surface. MS/BS: mineralizing surface per bone surface. Ob.S/BS: osteoblast surface per bone surface. MAR: mineral apposition rate. BFR/BS: bone formation rate per bone surface. Data are represented as mean ± SEM.

(C) Immunochemical identification of ERα (brown) in TRAP-positive (red) differentiated osteoclasts. The femurs of 12 week-old mice were used for the immunodetection of ERα in bone cells. All labels were abolished when the primary antibody was preadsorbed with the immunizing peptide (negative control).

The number of TRAP-positive osteoclasts differentiated from the bone-marrow cells of $ER\alpha^{\Delta Oc/\Delta Oc}$ females was almost the same as that from $ER\alpha^{+/+}$ females (Figure 5A) and males (data not shown). The differentiated $ER\alpha^{\Delta Oc/\Delta Oc}$ osteoclasts had typical osteoclastic features, including the characteristic cell shape, TRAP-positive, multiple nuclei, and actin-ring formation, and were indistinguishable from the $ER\alpha^{+/+}$ osteoclasts (Figure 5B).

The expression levels of the prime osteoclastogenic transcription factors, c-*fos* and *NFATc1*, were unaltered by ERα deficiency in differentiated osteoclasts (Figure 5C). Furthermore, responses to RANKL in intracellular signaling, as represented by phosphorylation of p38 and IκB, were unaffected in $ER\alpha^{\Delta Oc/\Delta Oc}$ osteoclasts from females (Figure 5D) as well as males (data not shown). In light of these findings, it is unlikely that activated ERα in osteoclastic cells attenuates osteoclastogenesis.

Activation of the Fas/FasL System by Estrogen in Intact Bone Is Impaired by Osteoclastic ERα Deficiency

To examine osteoclastic ERα function in intact bone, DNA microarray analysis following real-time RT-PCR of RNA from the femurs of ovariectomized $ER\alpha^{\Delta Oc/\Delta Oc}$ females treated with or without estrogen, was performed. During

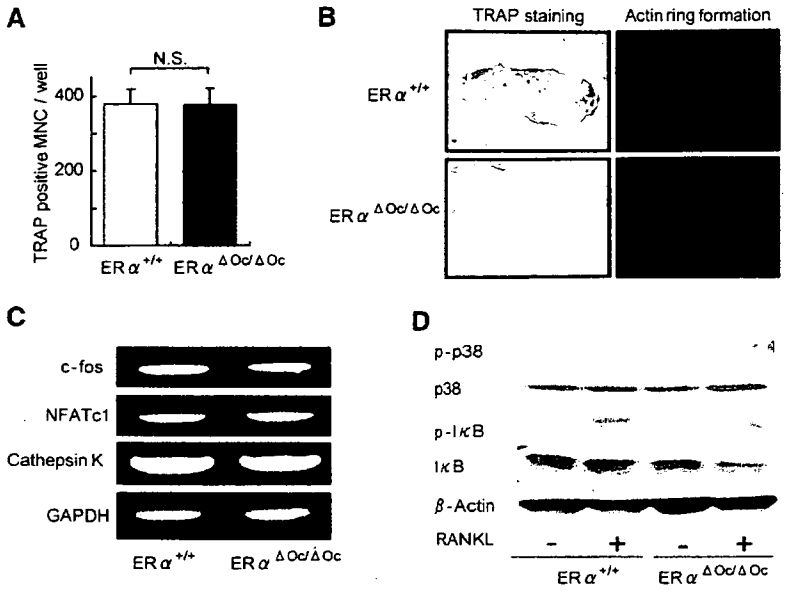

Figure 5. ERα Deficiency Did Not Affect Osteoclastogenesis

(A) TRAP-positive multinucleated cell count at 3 days after RANKL stimulation, cultured in 24-well plates (n = 6, N.S., not significant). Data are represented as mean ± SEM.

(B) TRAP staining and actin ring formation of RANKL induced primary cultured osteoclasts from bone-marrow cells of $ERα^{+/+}$ and $ERα^{ΔOc/ΔOc}$ mice.

(C) RT-PCR analysis of genes related to osteoclastogenesis.

(D) Western blot analysis of phosphorylated p38, JNK, and IκB of primary cultured bone-marrow cells stimulated with or without 100 ng/ml of RANKL for 15 min.

the search for candidate ERα target genes in bone by DNA microarray analysis (Figure S3), we found that a number of apoptosis-related factors were regulated by estrogen in the intact bone of $ERα^{+/+}$ females but dysregulated in $ERα^{ΔOc/ΔOc}$ females. This observation is consistent with a previous report of estrogen-induced apoptosis of mature osteoclasts (Kameda et al., 1997). Real-time RT-PCR to validate the estrogen regulations of the candidate genes revealed that gene expression of *FasL*, an apoptotic factor, was responsive to E2 (Figure 6A). Estrogen treatment (+E2) indeed induced expression of FasL protein in bone of ovariectomized $ERα^{+/+}$, but this induction was not obvious in ovariectomized $ERα^{ΔOc/ΔOc}$ mice (Figures 6B and 6C). Reflecting FasL induction by estrogen, estrogen-induced apoptosis (as observed by the TUNEL assay) in TRAP-positive mature trabecular osteoclasts in the distal femurs of the $ERα^{+/+}$ mice was detected, but this E2 response was abolished in the $ERα^{ΔOc/ΔOc}$ mice (Figure 6D). Furthermore, in mice lacking functional FasL ($FasL^{gld/gld}$), neither enhanced bone resorption nor bone mass loss was induced by ovariectomy (Figures 6E and 6F).

Osteoclastic ERα Mediates Estrogen-Induced apoptosis by FasL

The expression level of ERα protein in differentiated osteoclasts derived from bone marrow cells was very low, but induction of *FasL* gene expression was also detectable in the cultured osteoclasts of $ERα^{+/+}$ females as well as males (Figure 7A). However, this E2 response was impaired in cultured osteoclasts from $ERα^{ΔOc/ΔOc}$ females (Figure 7A). It is notable that such responses are also induced by tamoxifen (Figure 7C), which is an osteoprotective SERM (Harada and Rodan, 2003). ERα overexpression augmented *FasL* gene expression in response to estrogen in cultured osteoclasts from $ERα^{ΔOc/ΔOc}$ females (Figure S4A). In primary cultured calvarial osteoblasts from females as well as males (Suzawa et al., 2003), *FasL* gene induction by E2 and tamoxifen was also seen; however, it was not accompanied by increased apoptosis (data not shown). Thus, it appears that estrogen-induced apoptosis in osteoclasts is mediated by FasL expression in osteoclasts in the trabecular bone areas, presumably as well as in osteoblasts in cortical bone areas. As expected, the cell number of TUNEL-positive osteoclasts was increased by E2 in the cultured osteoclasts from $ERα^{+/+}$ females, but E2-induced apoptosis was undetectable in $ERα^{ΔOc/ΔOc}$ osteoclasts (Figure 7B). Consistent with FasL-induced apoptosis, *Fas* gene expression was observed (Figure 7D), but it was likely that Fas expression did not require ERα function (Figures S4B and S4C). Expression levels of *Fas* and *ERα* as well as E2 response in apoptosis appeared to fluctuate during osteoclast differentiation (Figures S4B–S4D); however, in FasL mutant ($FasL^{gld/gld}$) females, the E2-induced apoptosis was abolished (Figure S4E). These findings suggest that activated ERα in differentiated osteoclasts induces apoptosis through activating FasL/Fas signaling. This leads to suppression of bone resorption through truncating the already short life span of differentiated osteoclasts (Teitelbaum, 2006).

DISCUSSION

Selective ablation of ERα in mature osteoclasts in female mice shows that the osteoprotective effect of estrogen is mediated by osteoclastic ERα, at least in the trabecular regions of the tibiae, femur, and lumbar vertebrae of female mice. Activated ERα by estrogen as well as SERMs appears to truncate the already short life span (estimated at 2 weeks) of differentiated osteoclasts by inducing apoptosis through activation of the Fas/FasL system.

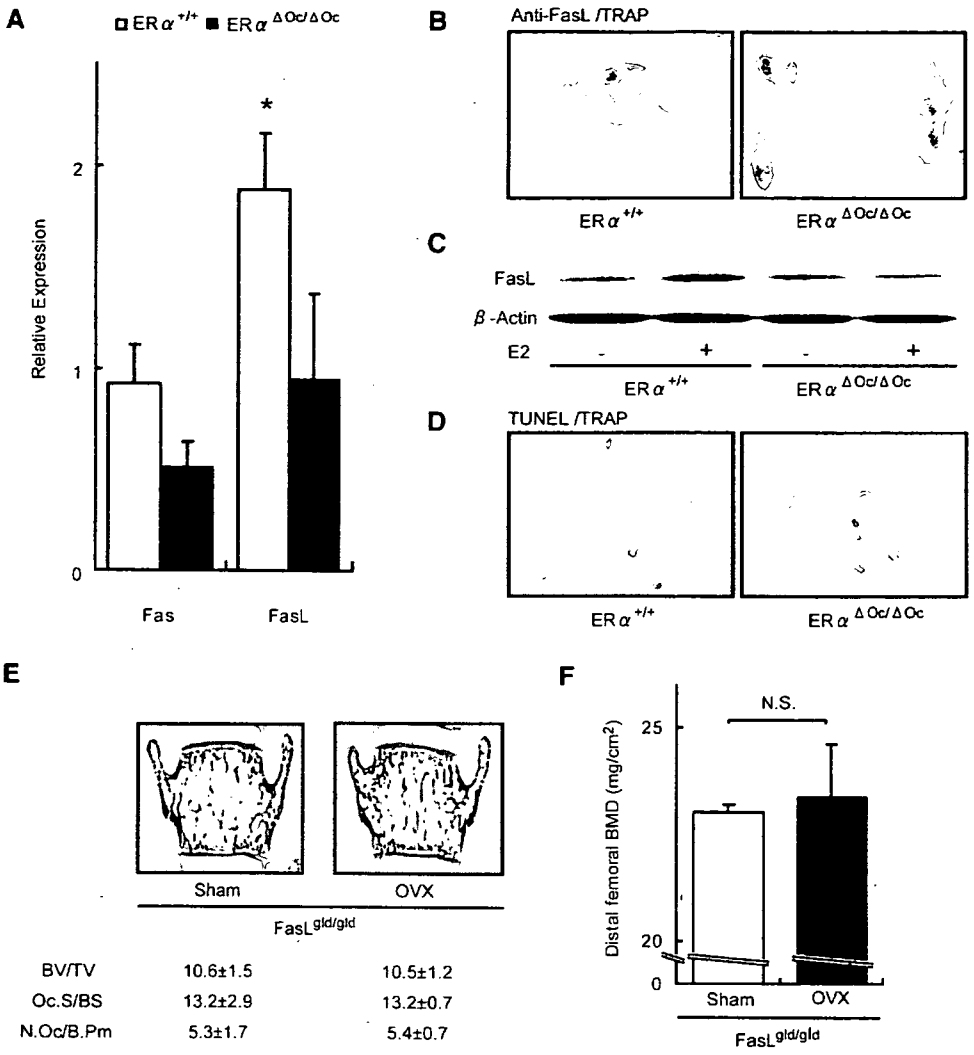

Figure 6. Activated ERα Induced Fas Ligand Expression and Apoptosis in Differentiated Osteoclasts of Intact Bone

(A) Real-time RT-PCR analysis of *Fas* and *FasL*. Expression levels in bones from E2-treated ovariectomized $ER\alpha^{+/+}$ (open column) and $ER\alpha^{\Delta Oc/\Delta Oc}$ (filled column) were compared with the ovariectomized groups of each genotype without E2 administration (*$p < 0.05$ compared to $ER\alpha^{+/+}$). Data are represented as mean ± SEM.

(B) Immunohistochemical analysis of anti-FasL with TRAP staining of the sections from the distal femurs of E2-treated ovariectomized $ER\alpha^{+/+}$ and $ER\alpha^{\Delta Oc/\Delta Oc}$ mice. Brawny stained cells are anti-FasL positive.

(C) Anti-FasL western blot analysis of proteins obtained from femurs of ovariectomized $ER\alpha^{+/+}$ and $ER\alpha^{\Delta Oc/\Delta Oc}$ mice treated with or without E2, using anti-β-actin as internal control.

(D) TUNEL staining with TRAP staining of the sections from the distal femurs of E2-treated ovariectomized $ER\alpha^{+/+}$ and $ER\alpha^{\Delta Oc/\Delta Oc}$ mice. Arrowheads indicate both TUNEL (brown)- and TRAP-positive staining cells.

(E) Bone histomorphometrical analysis of sham-operated or ovariectomized $FasL^{gld/gld}$ mice.

(F) BMD of the distal femurs of sham operated or ovariectomized $FasL^{gld/gld}$ mice. Data are represented as mean ± SEM.

This attenuates bone resorption. This idea is supported by previous observations that estrogen deficiency following menopause or ovariectomy leads to high bone turnover, particularly in the trabecular areas, as bone is rapidly lost through enhanced resorption (Delmas, 2002; Tolar et al., 2004). Thus, estrogen treatment leads to recovery from osteopenia by reducing resorption (Delmas, 2002; Rodan and Martin, 2000), partly by the induction of osteoclast cell death.

In contrast to the osteopenia seen in the $ER\alpha^{\Delta Oc/\Delta Oc}$ females, the $ER\alpha^{\Delta Oc/\Delta Oc}$ male mice unexpectedly had no bone loss. The male mice still demonstrated an ERα-mediated induction of FasL in response to estrogen with subsequent apoptosis of osteoclasts (Figure 7). Both male mice with a deficiency of aromatase that are unable to locally produce estrogen from testosterone and men with a genetic mutation in the *ERα* gene suffer from osteoporosis (Smith et al., 1994). Considering that the

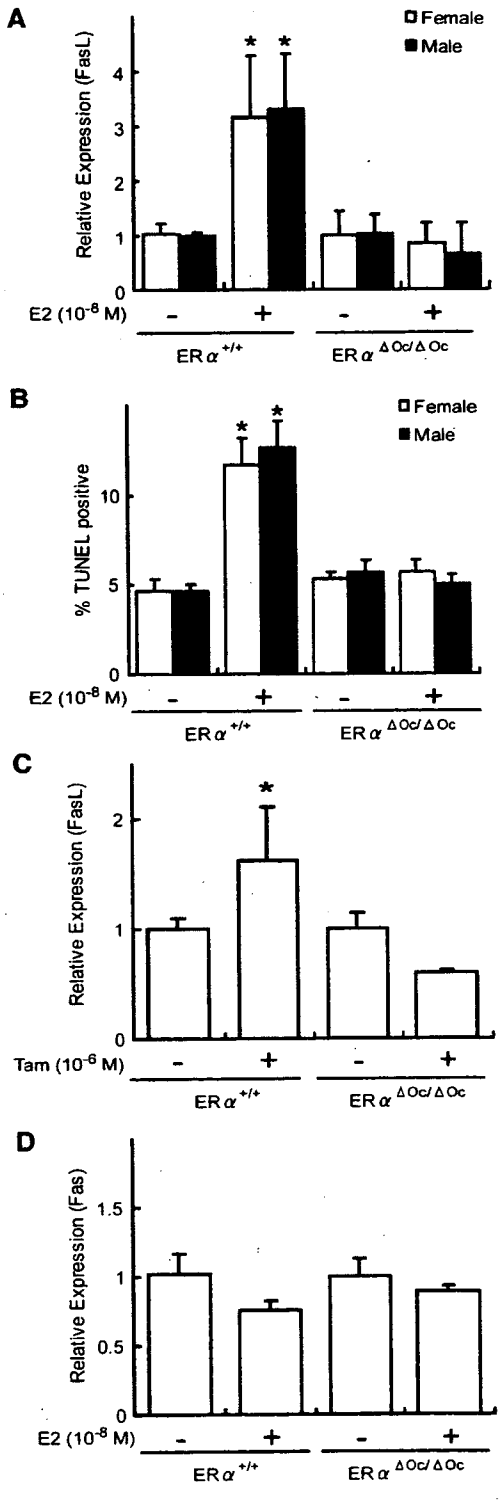

Figure 7. Estrogen-Induced *FasL* Expression and Apoptosis Required ERα in Cultured Osteoclasts

(A) Real-time RT-PCR analysis of *FasL* expression using total RNA obtained from in vitro primary cultured osteoclasts of each genotype at 3 days after RANKL stimulation, treated with or without E2 (10^{-8} M) for 4 hr (*$p < 0.05$ compared to the group treated without E2). Data are represented as mean ± SEM.

(B) Apoptotic cells were defined as those with TUNEL-positive nuclei among TRAP-positive multinucleated primary cultured osteoclasts treated with or without E2 (10^{-8} M) for 12 hr in 96-well plates (*$p < 0.05$ compared to the group treated without E2). Data are represented as mean ± SEM.

(C) *FasL* expression in each genotypic female osteoclastic cells treated with or without Tam (10^{-6} M) (*$p < 0.05$ compared to the group treated without Tam). Data are represented as mean ± SEM.

(D) Expression of *Fas* was measured as described in the legend of Figure 7A. Data are represented as mean ± SEM.

markedly elevated levels of testosterone in ERα KO females may be potent enough to maintain normal bone turnover (Syed and Khosla, 2005), it is likely that the activated AR might be functionally sufficient in male mice to compensate for the ERα deficiency in bone (Kawano et al., 2003). However, species differences in the osteoprotective action of sex steroid hormones still need to be carefully addressed.

Fas/FasL system-mediated apoptotic induction of osteoclasts by estrogen may well be a part of the mechanism for the antiresorptive action of estrogen and SERMs in trabecular bone areas (Delmas, 2002; Rodan and Martin, 2000; Simpson and Davis, 2001; Syed and Khosla, 2005; Tolar et al., 2004). Regulation of osteoclast differentiation is tightly coupled to osteoblastic function in terms of cytokine production and cell-cell contact (Karsenty and Wagner, 2002; Martin and Sims, 2005; Mundy and Elefteriou, 2006; Teitelbaum and Ross, 2003). Indeed, upregulation of osteoclastogenic cytokines by ovariectomy was unaffected in $ER\alpha^{\Delta Oc/\Delta Oc}$ females. Considering the observation that cortical bone mass is increased in ovariectomized $ER\alpha^{\Delta Oc/\Delta Oc}$ females during estrogen treatment, it is conceivable that the antiresorptive estrogen action in cortical bone is also mediated by osteoblastic ERα. In this regard, FasL induction by estrogen in osteoblasts may contribute to the osteoprotective estrogen action, and *FasL* gene induction by estrogen was in fact detected in primary cultured osteoblasts from female calvaria by us as well as another group (S. Krum and M. Brown, personal communication). Thus, similar experiments in which ERα is selectively ablated in osteoblasts are needed to define the role of ERα in these cells.

In osteoclastic cells, expression of the *FasL* gene, which leads to apoptosis, appears to be positive controlled by activated ERα. Not surprisingly, a direct binding site for ERα has been mapped in the *FasL* gene locus (S. Krum and M. Brown, personal communication). An osteoclast- and cell-differentiation stage-specific mechanism may underlie this gene induction in the *FasL* gene promoter. A recent study demonstrated that ERα recruitment to specific promoter sites of given ERα target genes was cell-type specific (Carroll et al., 2005). Thus, there is significant impetus to identify the osteoclastic factor that associates with ERα in the *FasL* gene promoter. Such identification will lead to a better understanding of the molecular basis of the osteoprotective estrogen action and provide a target against which to develop SERMs of greater effectiveness.

EXPERIMENTAL PROCEDURES

Ctsk-Cre Construction and Generation of the Knockin Mouse Lines

An RP23-422n18 BAC clone containing the mouse *Ctsk* gene was purchased from Invitrogen (Carlsbad, CA). The *FRT-Kan*^{r}*/Neo*^{r}*-FRT* and *nlsCre* fragments were obtained from plasmids pSK2/3-*FRT-Neo* and pIC-*Cre*. Two homologous arms of 500 bp from the *Ctsk* gene were inserted into both sides of the *nlsCre-FRT-Kan*^{r}*/Neo*^{r}*-FRT* cassette in the pSK2/3-*FRT-Neo* plasmid. The *nlsCre-FRT-Kan*^{r}*/Neo*^{r}*-FRT* cassette was introduced into the endogenous ATG start site of the *Ctsk* gene by recombineering approaches (Copeland et al., 2001). Targeted BAC was reduced in size from 189 kb to 26 kb and subcloned into the pMC1-DTpA vector by the gap-repair method. The targeted TT2 ES clones were selected after positive-negative selection with G418 and DT-A with Southern analysis, then aggregated with single eight-cell embryos from CD-1 mice (Yoshizawa et al., 1997). Chimeric mice were then crossed with a general deleter mouse line, *ACTB-Flpe* (Jackson Laboratory), to remove the *Kan*^{r}*/Neo*^{r} cassette. The *Ctsk-Cre* mice (*Ctsk*$^{Cre/+}$), originally on a hybrid C57BL/6 and CBA genetic background, were backcrossed for four generations into a C57BL/6J background. *FasL*$^{gld/gld}$ mice were also purchased from Jackson Laboratory.

Analysis of Cre Recombinase Activities

Expression of the Cre transcript was detected by RT-PCR. Southern analysis using a *Cre* cDNA probe was performed with total RNA extracted from 12-week-old mice. To evaluate the specificity and efficiency of Cre-mediated recombination, we mated the *Ctsk*$^{Cre/+}$ mice to *CAG-CAT-Z* reporter mice (kindly provided by J. Miyazaki) (Sakai and Miyazaki, 1997) and genotyped their offspring with *Cre*-specific primers. β-galactosidase activity of the expressed *LacZ* gene driven by the *CAG* promoter was expected to be detected in the given cells expressing functional Cre recombinase.

In Vitro Osteoclastogenesis and Ligand Application

Bone-marrow cells derived from 8-week-old mice were plated in culture dishes containing α-MEM (GIBCO-BRL) with 10% FBS (JRH) and 10 ng/ml M-CSF (Genzyme). After incubation for 48 hr, adherent cells were used as osteoclast precursor cells after washing out the nonadherent cells. Cells were cultured in the presence of 10 ng/ml M-CSF and 100 ng/ml RANKL (Peprotech) to generate osteoclast-like cells (Koga et al., 2004) for 3 days, so the total culture time was 5 days. Three days after RANKL stimulation, primary cultured osteoclasts were treated with 10^{-8} M of 17β-estradiol (E2) (Sigma-Aldrich Co.) or 10^{-6} M 4-hydroxytamoxifen (Tam) (Sigma-Aldrich Co.) in phenol-red free medium.

Generation of Osteoclast-Specific ERα KO Mice

The ERα conditional (*ERα*$^{flox/flox}$) (Dupont et al., 2000) and null alleles with a C57BL/6J background have been previously described. *ERα*$^{flox/flox}$ mice were crossed with *Ctsk*$^{Cre/+}$ mice to generate *Ctsk*$^{Cre/+}$; *ERα*$^{flox/+}$ mice. *Ctsk*$^{Cre/+}$; *ERα*$^{+/+}$ (*ERα*$^{+/+}$) and *Ctsk*$^{Cre/+}$; *ERα*$^{flox/flox}$ (*ERα*$^{\Delta Oc/\Delta Oc}$) mice were obtained by crossing *Ctsk*$^{Cre/+}$; *ERα*$^{flox/+}$ with *ERα*$^{flox/+}$ mouse lines.

Radiological Analysis

Bone radiographs of the femurs of 12-week-old *Ctsk*$^{Cre/+}$; *ERα*$^{flox/flox}$ (*ERα*$^{\Delta Oc/\Delta Oc}$) and *Ctsk*$^{Cre/+}$; *ERα*$^{+/+}$ (*ERα*$^{+/+}$) littermates were visualized with a soft X-ray apparatus (TRS-1005: SOFTRON). BMD was measured by DXA using a bone mineral analyzer (DCS-600EX: ALOKA). Micro Computed Tomography scanning of the femurs was performed using a composite X-ray analyzer (NX-CP-C80H-IL: Nittetsu ELEX Co.) (Kawano et al., 2003). Tomograms were obtained with a slice thickness of 10 μm and reconstructed at 12 × 12 pixels into a 3D image by the volume-rending method (VIP-Station; Teijin System Technology) using a computer.

Analysis of Skeletal Morphology

Twelve-week-old *Ctsk*$^{Cre/+}$; *ERα*$^{flox/flox}$ (*ERα*$^{\Delta Oc/\Delta Oc}$) and *Ctsk*$^{Cre/+}$; *ERα*$^{+/+}$ (*ERα*$^{+/+}$) littermates were double labeled with subcutaneous injections of 16 mg/kg of calcein (Sigma) at 4 and 2 days before sacrifice. Tibiae were removed from each mouse and fixed with 70% ethanol. They were stained with Villanueva bone stain for 7 days and embedded in methyl-methacrylate (Wako) (Yoshizawa et al., 1997). Frontal plane sections (5-μm thick) of the proximal tibia were cut using a Microtome (LEICA). The cancellous bone was measured in the secondary spongiosa located 500 μm from the epiphyseal growth plate and 160 μm from the endocortical surface (Kawano et al., 2003; Nakamichi et al., 2003). Bone histomorphometric measurements of the tibia were made using a semiautomatic image analyzing system (System Supply) and a fluorescent microscope (Optiphot; Nikon). Similar measurements of the lumbar vertebral bodies were done as previously reported (Takeda et al., 2002). Standard bone histomorphometrical nomenclatures, symbols, and units were used as described in the report of the ASBMR Histomophometry Nomenclature Committee.

Ovariectomy and Hormone Replacement

Female *Ctsk*$^{Cre/+}$; *ERα*$^{flox/flox}$ (*ERα*$^{\Delta Oc/\Delta Oc}$) and *Ctsk*$^{Cre/+}$; *ERα*$^{+/+}$ (*ERα*$^{+/+}$) littermates were ovariectomized or sham operated at 8–12 weeks of age for 2 weeks for all experiments, and slow releasing pellets of E2 (0.83 μg/day) or placebo (Innovative Research, Sarasota, FL) were implanted subcutaneously in the scapular region behind the neck (Sato et al., 2004; Shiina et al., 2006).

Immunohistochemistry

Twelve-week-old *Ctsk*$^{Cre/+}$; *ERα*$^{flox/flox}$ (*ERα*$^{\Delta Oc/\Delta Oc}$) and *Ctsk*$^{Cre/+}$; *ERα*$^{+/+}$ (*ERα*$^{+/+}$) littermates were fixed with 4% PFA by perfusion. Serial sections of the brain (20 μm thick) were divided into two groups and used for single labeling for the ERα or thionin to allow determination of the areas to be measured. Tibiae and femurs were decalcified in 10% EDTA for 2–4 weeks after fixation and then embedded in paraffin sections. Sections were incubated in L.A.B. solution (Polysciences) for 30 min to retrieve antigen. The cooled sections were incubated in 1% H_2O_2 for 30 min to quench endogenous peroxidase and then washed with 1% Triton X-100 in PBS for 10 min. To block nonspecific antibody binding, sections were incubated in blocking solution (DAKO) for 5 min. Sections were then incubated with anti-ERα (Santa Cruz, CA) and anti-FasL (Santa Cruz, CA) in blocking solution overnight at 4°C. Staining was then performed using the EnVision+ HRP System (Dako) and 3, 3′-diaminobendizine tetrahydrochloride substrate (Sigma), counterstained with TRAP, dehydrated through an ethanol series and xylene, before mounting (Sato et al., 2004).

ERα Overexpression

Two days after RANKL stimulation, an expression vector of mouse ERα was tranfected into immature osteoclastic cells from *ERα*$^{\Delta Oc/\Delta Oc}$ mice using Superfect (QIAGEN) as manufacture's instruction.

Real-Time RT-PCR

One microgram of total RNA from each sample was reverse transcribed into first-strand cDNA with random hexamers using Superscript III reverse transcriptase (Invitrogen). Primer sets for all genes were purchased from Takara Bio. Inc. (Tokyo, Japan). Real-time RT-PCR was performed using SYBR Premix Ex Taq (Takara) with the ABI PRISM 7900HT (Applied Biosystems) according to the manufacturer's instructions. Experimental samples were matched to a standard curve generated by amplifying serially diluted products using the same PCR protocol. To correct for variability in RNA recovery and efficiency of reverse transcription, *Gapdh* cDNA was amplified and quantified in each cDNA preparation. Normalization and calculation steps were performed as reported previously (Takezawa et al., 2007).

TUNEL/TRAP Staining

The TUNEL method was performed using the ApopTag Fluorescein In Situ Apoptosis Detection Kit (CHEMICON international) according to the manufacturer's instructions with a slight modification. This was followed by TRAP staining as previously reported (Kobayashi et al., 2000).

Cytokine Assays

Bone marrow and blood were collected at 2 weeks after sham operation or ovariectomy. Bone-marrow cells were cultured for 3 days in DMEM. The levels of TNFα, IL-1α, and IL-6 in the culture media and serum RANKL were determined by ELISA (R&D Systems).

Western Blot

Osteoclast precursor cells were treated with or without 100 ng/ml of soluble RANKL. After 15 minutes, cell extracts were harvested from the cells using lysis buffer containing 100 mM Tris-HCl (pH 7.8), 150 mM NaCl, 0.1% Triton X-100, 5% protease inhibitor cocktail (Sigma), and 5% phosphatase inhibitor cocktail (Sigma). An equivalent amount of protein from each of the cell extracts and proteins of femoral bone extracted using ISOGEN was loaded for SDS-PAGE and transferred to PVDF membranes (Amersham Biosciences). The membranes were developed with enhanced chemiluminescence reagent (Amersham Biosciences) (Ohtake et al., 2003). Phosphorylation of p38 MAPK and IκB were evaluated using antibodies purchased from Cell Signaling Technology (Koga et al., 2004) and anti-FasL antibody was purchased from Santa Cruz Biotechnology (sc-834).

Actin-Ring Formation

Cells were fixed for 15 min in warm 4% paraformaldehyde (PFA). After fixation, cells were washed three times with PBS with 0.1% Triton X-100 (PBST) and incubated with 0.2 U/ml rhodamine phalloidin (Molecular Probes) for 30 min and washed again three times in PBST.

Statistical Analysis

Data were analyzed by two-tailed student's t test. For all graphs, data are represented as mean ± SEM.

Supplemental Data

Supplemental Data include Supplemental Experimental Procedures and four figures and can be found with this article online at http://www.cell.com/cgi/content/full/130/5/811/DC1/.

ACKNOWLEDGMENTS

We thank Drs. S. Krum and M. Brown to share with their unpublished results; Drs. K. Yoshimura, Y. Nakamichi, T. Watanabe, J. Miyamoto, H. Shiina, T. Fukuda, Ms. Y. Sato, and S. Tanaka for generation of the KO mice; Drs. T. Koga, H. Takagi, E. Ochiai, and N. Moriyama for technical help; Dr. J. Miyazaki for *CAG-CAT-Z* reporter mice, and H. Higuchi and K. Hiraga for manuscript preparation. This work was supported in part by priority areas from the Ministry of Education, Culture, Sports, Science and Technology (to S.K.) and the Program for Promotion of Basic Research Activities for Innovative Biosciences (PROBRAIN).

Received: February 23, 2007
Revised: May 21, 2007
Accepted: July 17, 2007
Published: September 6, 2007

REFERENCES

Belandia, B., and Parker, M.G. (2003). Nuclear receptors: a rendezvous for chromatin remodeling factors. Cell *114*, 277–280.

Bland, R. (2000). Steroid hormone receptor expression and action in bone. Clin. Sci. (Lond.) *98*, 217–240.

Carroll, J.S., Liu, X.S., Brodsky, A.S., Li, W., Meyer, C.A., Szary, A.J., Eeckhoute, J., Shao, W., Hestermann, E.V., Geistlinger, T.R., et al. (2005). Chromosome-wide mapping of estrogen receptor binding reveals long-range regulation requiring the forkhead protein FoxA1. Cell *122*, 33–43.

Chien, K.R., and Karsenty, G. (2005). Longevity and lineages: toward the integrative biology of degenerative diseases in heart, muscle, and bone. Cell *120*, 533–544.

Copeland, N.G., Jenkins, N.A., and Court, D.L. (2001). Recombineering: a powerful new tool for mouse functional genomics. Nat. Rev. Genet. *2*, 769–779.

Couse, J.F., and Korach, K.S. (1999). Estrogen receptor null mice: what have we learned and where will they lead us? Endocr. Rev. *20*, 358–417.

Delmas, P.D. (2002). Treatment of postmenopausal osteoporosis. Lancet *359*, 2018–2026.

Dupont, S., Krust, A., Gansmuller, A., Dierich, A., Chambon, P., and Mark, M. (2000). Effect of single and compound knockouts of estrogen receptors alpha (ERalpha) and beta (ERbeta) on mouse reproductive phenotypes. Development *127*, 4277–4291.

Gowen, M., Lazner, F., Dodds, R., Kapadia, R., Feild, J., Tavaria, M., Bertoncello, I., Drake, F., Zavarselk, S., Tellis, I., et al. (1999). Cathepsin K knockout mice develop osteopetrosis due to a deficit in matrix degradation but not demineralization. J. Bone Miner. Res. *14*, 1654–1663.

Harada, S., and Rodan, G.A. (2003). Control of osteoblast function and regulation of bone mass. Nature *423*, 349–355.

Kameda, T., Mano, H., Yuasa, T., Mori, Y., Miyazawa, K., Shiokawa, M., Nakamaru, Y., Hiroi, E., Hiura, K., Kameda, A., et al. (1997). Estrogen inhibits bone resorption by directly inducing apoptosis of the bone-resorbing osteoclasts. J. Exp. Med. *186*, 489–495.

Karsenty, G. (2006). Convergence between bone and energy homeostases: leptin regulation of bone mass. Cell Metab. *4*, 341–348.

Karsenty, G., and Wagner, E.F. (2002). Reaching a genetic and molecular understanding of skeletal development. Dev. Cell *2*, 389–406.

Kato, S., Ito, S., Noguchi, T., and Naito, H. (1989). Effects of brefeldin A on the synthesis and secretion of egg white proteins in primary cultured oviduct cells of laying Japanese quail (Coturnix coturnix japonica). Biochim. Biophys. Acta *991*, 36–43.

Kawano, H., Sato, T., Yamada, T., Matsumoto, T., Sekine, K., Watanabe, T., Nakamura, T., Fukuda, T., Yoshimura, K., Yoshizawa, T., et al. (2003). Suppressive function of androgen receptor in bone resorption. Proc. Natl. Acad. Sci. USA *100*, 9416–9421.

Kimble, R.B., Matayoshi, A.B., Vannice, J.L., Kung, V.T., Williams, C., and Pacifici, R. (1995). Simultaneous block of interleukin-1 and tumor necrosis factor is required to completely prevent bone loss in the early postovariectomy period. Endocrinology *136*, 3054–3061.

Kobayashi, Y., Hashimoto, F., Miyamoto, H., Kanaoka, K., Miyazaki-Kawashita, Y., Nakashima, T., Shibata, M., Kobayashi, K., Kato, Y., and Sakai, H. (2000). Force-induced osteoclast apoptosis in vivo is accompanied by elevation in transforming growth factor beta and osteoprotegerin expression. J. Bone Miner. Res. *15*, 1924–1934.

Koga, T., Inui, M., Inoue, K., Kim, S., Suematsu, A., Kobayashi, E., Iwata, T., Ohnishi, H., Matozaki, T., Kodama, T., et al. (2004). Costimulatory signals mediated by the ITAM motif cooperate with RANKL for bone homeostasis. Nature *428*, 758–763.

Li, C.Y., Jepsen, K.J., Majeska, R.J., Zhang, J., Ni, R., Gelb, B.D., and Schaffler, M.B. (2006). Mice lacking Cathepsin K maintain bone remodeling but develop bone fragility despite high bone mass. J. Bone Miner. Res. *21*, 865–875.

Mangelsdorf, D.J., Thummel, C., Beato, M., Herrlich, P., Schutz, G., Umesono, K., Blumberg, B., Kastner, P., Mark, M., Chambon, P., and Evans, R.M. (1995). The nuclear receptor superfamily: the second decade. Cell *83*, 835–839.

Martin, T.J., and Sims, N.A. (2005). Osteoclast-derived activity in the coupling of bone formation to resorption. Trends Mol. Med. *11*, 76–81.

Mueller, S.O., and Korach, K.S. (2001). Estrogen receptors and endocrine diseases: lessons from estrogen receptor knockout mice. Curr. Opin. Pharmacol. *1*, 613–619.

Mundy, G.R., and Elefteriou, F. (2006). Boning up on ephrin signaling. Cell *126*, 441–443.

Nakamichi, Y., Shukunami, C., Yamada, T., Aihara, K., Kawano, H., Sato, T., Nishizaki, Y., Yamamoto, Y., Shindo, M., Yoshimura, K., et al. (2003). Chondromodulin I is a bone remodeling factor. Mol. Cell. Biol. *23*, 636–644.

Ohtake, F., Takeyama, K., Matsumoto, T., Kitagawa, H., Yamamoto, Y., Nohara, K., Tohyama, C., Krust, A., Mimura, J., Chambon, P., et al. (2003). Modulation of oestrogen receptor signalling by association with the activated dioxin receptor. Nature *423*, 545–550.

Raisz, L.G. (2005). Pathogenesis of osteoporosis: concepts, conflicts, and prospects. J. Clin. Invest. *115*, 3318–3325.

Riggs, B.L., and Hartmann, L.C. (2003). Selective estrogen-receptor modulators–mechanisms of action and application to clinical practice. N. Engl. J. Med. *348*, 618–629.

Rodan, G.A., and Martin, T.J. (2000). Therapeutic approaches to bone diseases. Science *289*, 1508–1514.

Saftig, P., Hunziker, E., Wehmeyer, O., Jones, S., Boyde, A., Rommerskirch, W., Moritz, J.D., Schu, P., and von Figura, K. (1998). Impaired osteoclastic bone resorption leads to osteopetrosis in Cathepsin-K-deficient mice. Proc. Natl. Acad. Sci. USA *95*, 13453–13458.

Sakai, K., and Miyazaki, J. (1997). A transgenic mouse line that retains Cre recombinase activity in mature oocytes irrespective of the cre transgene transmission. Biochem. Biophys. Res. Commun. *237*, 318–324.

Sato, T., Matsumoto, T., Kawano, H., Watanabe, T., Uematsu, Y., Sekine, K., Fukuda, T., Aihara, K., Krust, A., Yamada, T., et al. (2004). Brain masculinization requires androgen receptor function. Proc. Natl. Acad. Sci. USA *101*, 1673–1678.

Shang, Y., and Brown, M. (2002). Molecular determinants for the tissue specificity of SERMs. Science *295*, 2465–2468.

Shiina, H., Matsumoto, T., Sato, T., Igarashi, K., Miyamoto, J., Takemasa, S., Sakari, M., Takada, I., Nakamura, T., Metzger, D., et al. (2006). Premature ovarian failure in androgen receptor-deficient mice. Proc. Natl. Acad. Sci. USA *103*, 224–229.

Simpson, E.R., and Davis, S.R. (2001). Minireview: aromatase and the regulation of estrogen biosynthesis–some new perspectives. Endocrinology *142*, 4589–4594.

Sims, N.A., Clement-Lacroix, P., Minet, D., Fraslon-Vanhulle, C., Gaillard-Kelly, M., Resche-Rigon, M., and Baron, R. (2003). A functional androgen receptor is not sufficient to allow estradiol to protect bone after gonadectomy in estradiol receptor-deficient mice. J. Clin. Invest. *111*, 1319–1327.

Smith, E.P., Boyd, J., Frank, G.R., Takahashi, H., Cohen, R.M., Specker, B., Williams, T.C., Lubahn, D.B., and Korach, K.S. (1994). Estrogen resistance caused by a mutation in the estrogen-receptor gene in a man. N. Engl. J. Med. *331*, 1056–1061.

Sun, L., Peng, Y., Sharrow, A.C., Iqbal, J., Zhang, Z., Papachristou, D.J., Zaidi, S., Zhu, L.L., Yaroslavskiy, B.B., Zhou, H., et al. (2006). FSH directly regulates bone mass. Cell *125*, 247–260.

Suzawa, M., Takada, I., Yanagisawa, J., Ohtake, F., Ogawa, S., Yamauchi, T., Kadowaki, T., Takeuchi, Y., Shibuya, H., Gotoh, Y., et al. (2003). Cytokines suppress adipogenesis and PPAR-gamma function through the TAK1/TAB1/NIK cascade. Nat. Cell Biol. *5*, 224–230.

Syed, F., and Khosla, S. (2005). Mechanisms of sex steroid effects on bone. Biochem. Biophys. Res. Commun. *328*, 688–696.

Takeda, S., Elefteriou, F., Levasseur, R., Liu, X., Zhao, L., Parker, K.L., Armstrong, D., Ducy, P., and Karsenty, G. (2002). Leptin regulates bone formation via the sympathetic nervous system. Cell *111*, 305–317.

Takezawa, S., Yokoyama, A., Okada, M., Fujiki, R., Iriyama, A., Yanagi, Y., Ito, H., Takada, I., Kishimoto, M., Miyajima, A., et al. (2007). A cell cycle-dependent co-repressor mediates photoreceptor cell-specific nuclear receptor function. EMBO J. *26*, 764–774.

Teitelbaum, S.L. (2006). Osteoclasts; culprits in inflammatory osteolysis. Arthritis Res. Ther. *8*, 201.

Teitelbaum, S.L. (2007). Osteoclasts: what do they do and how do they do it? Am. J. Pathol. *170*, 427–435.

Teitelbaum, S.L., and Ross, F.P. (2003). Genetic regulation of osteoclast development and function. Nat. Rev. Genet. *4*, 638–649.

Tolar, J., Teitelbaum, S.L., and Orchard, P.J. (2004). Osteopetrosis. N. Engl. J. Med. *351*, 2839–2849.

Windahl, S.H., Andersson, G., and Gustafsson, J.A. (2002). Elucidation of estrogen receptor function in bone with the use of mouse models. Trends Endocrinol. Metab. *13*, 195–200.

Yoshizawa, T., Handa, Y., Uematsu, Y., Takeda, S., Sekine, K., Yoshihara, Y., Kawakami, T., Arioka, K., Sato, H., Uchiyama, Y., et al. (1997). Mice lacking the vitamin D receptor exhibit impaired bone formation, uterine hypoplasia and growth retardation after weaning. Nat. Genet. *16*, 391–396.

Zaman, G., Jessop, H.L., Muzylak, M., De Souza, R.L., Pitsillides, A.A., Price, J.S., and Lanyon, L.L. (2006). Osteocytes use estrogen receptor alpha to respond to strain but their ERalpha content is regulated by estrogen. J. Bone Miner. Res. *21*, 1297–1306.

Accession Numbers

Microarray can be seen in Gene Expression Omnibus under accession number GSE7798.

Increased Hepatic Cytochrome P4503A Activity Decreases the Risk of Developing Steroid-Induced Osteonecrosis in a Rabbit Model

Toshiaki Masada,[1] Kentaro Iwakiri,[1] Yutaka Oda,[2] Yasunori Kaneshiro,[1] Hiroyoshi Iwaki,[1] Hirotsugu Ohashi,[1] Kunio Takaoka[1]

[1]Department of Orthopaedic Surgery, Osaka City University Graduate School of Medicine, Osaka City, Japan

[2]Department of Anesthesiology and Intensive Care Medicine, Osaka City University Graduate School of Medicine, Osaka City, Japan

Received 2 April 2007; accepted 18 June 2007

Published online 4 September 2007 in Wiley InterScience (www.interscience.wiley.com). DOI 10.1002/jor.20484

ABSTRACT: Low hepatic cytochrome P4503A (CYP3A) activities might play an important role for inducing osteonecrosis of the femoral head (ONFH) by corticosteroids. However, the relationship between hepatic CYP3A activity and steroid-induced ONFH is unknown. We have examined the relationship between hepatic CYP3A activity and the inducibility of ONFH in a rabbit model. Sixty rabbits were divided into three groups. Hepatic CYP3A inducer (phenobarbital, group P; $n = 15$), inhibitor (itraconazole, group I; $n = 15$), or saline (group C, $n = 30$) was administrated for 3 weeks before intramuscular methylprednisolone. In groups P and I, hepatic CYP3A levels were measured by midazolam clearance before treatment (baseline) and before methylprednisolone injection. All animals were sacrificed 3 weeks after methylprednisolone injection and both femurs were harvested and examined histologically for osteonecrosis. Midazolam clearance was significantly increased and decreased, compared with baseline in groups P and I respectively ($p < 0.0005$, $p < 0.002$). The incidence of osteonecrosis in group P (33%) was significantly lower than in group I (100%) and group C (83%; $p < 0.001$ for both). The percentage necrotic area to whole bone marrow area on cross sections in group P ($8.2 \pm 5.9\%$) was significantly lower than in group I ($69.8 \pm 20.8\%$) and group C ($51.5 \pm 30.7\%$; $p < 0.005$ for both). Hepatic CYP3A activity inversely correlated with the incidence of osteonecrosis and extent of the necrotic area caused by the same dose of corticosteroids, suggesting possible prevention of the steroid-induced osteonecrosis by reducing steroid dose in poor corticosteroid metabolizers. © 2007 Orthopaedic Research Society. Published by Wiley Periodicals, Inc. J Orthop Res 26:91–95, 2008

Keywords: CYP3A; osteonecrosis; animal model

INTRODUCTION

Osteonecrosis of the femoral head (ONFH) is one of the most serious complications induced by corticosteroid therapy.[1] In patients with ONFH, collapse of femoral head often occurs and causes severe hip pain and impaired hip joint function. Most of the ONFH patients require surgical treatment such as core decompression, osteotomy or total hip arthroplasty depending on stages of the progression of destruction of the hip joints. Despite the widely spread use of corticosteroids for treating various diseases[2–4] and a known association between prevalence of ONFH and daily dose of corticosteroids, pathomechanism for the development of ONFH has not been identified.

Because hepatic cytochrome P4503A (CYP3A) is a predominant enzyme responsible for metabolizing the corticosteroids[5–7] and its activities varies more than 10-fold,[8–10] low hepatic CYP3A activity leads to a remarkable increase of corticosteroid levels and its effect.[7] Because hepatic CYP3A levels are significantly lower in patients with steroid-induced ONFH,[11] increased levels of steroids might lead to adverse events including bone necrosis.

In the present study, we have examined the contribution of low CYP3A activity to the development of ONFH by manipulating the hepatic CYP3A activity with an inducer[12] and inhibitor[13] in a rabbit model. Unlike typical ONFH characterized by bone and marrow lesions localized predominantly in proximal part of the femur, widely distributed necrotic lesions in the skeleton

Correspondence to: Kentaro Iwakiri (Telephone: 81-6-6645-3851; Fax: 81-6-6646-6260;
E-mail: kentucky@msic.med.osaka-cu.ac.jp)

observed in this model may limit the use of this model as ONFH.[14] Despite these differences; however, it has extensively been used as a model for evaluating the risk factor and the prophylaxis of osteonecrosis.[15–19] This study was aimed at understanding whether the level of hepatic CYP3A activity is associated with a propensity to develop bone necrosis elicited by externally administrated steroid or not.

MATERIALS AND METHODS

All experiments were conducted in accordance with the guidelines for Animal Care and Experiments of Osaka City University, Osaka, Japan.

Animals

A total of 60 adult female Japanese white rabbits (Japan SLC Inc.; Shizuoka, Japan) ranging from 28 to 32 weeks were used in the studies. Each rabbit was housed in separate cage at the Animal Center in Osaka City University with free access to water and standard food. The body weights of the rabbits were measured every week over the experimental period.

Experimental Protocols

The animals were randomly divided into three groups. The first group received daily intramuscular phenobarbital (Daiichi-Sankyo, Tokyo, Japan; 25 mg/kg) to induce hepatic CYP3A for 6 weeks (group P; $n=15$). The second group received oral itraconazole (Meiji-Seika, Tokyo, Japan; 50 mg/kg) every other day to inhibit CYP3A activity (group I; $n=15$), and control group was treated with saline (group C; $n=30$). In groups P and I, before treating with phenobarbital and itraconazole (baseline) and 3 weeks later, hepatic CYP3A activity was assayed by midazolam clearance test as reported previously.[20] In brief, under general anesthesia with intramuscular ketamine (10 mg/kg) and xylazine (1.2 mg/kg), midazolam (0.5 mg/kg) was administrated intravenously through the auricular vein. One milliliterl of blood samples were collected at 5, 10, 15, 20, 30, 45, 60, 90, 120, 180, and 240 min after midazolam injection. Plasma concentration of midazolam was measured by one of the authors (YO), who was unaware of the group allocation. Clearance of midazolam was calculated by the dose divided by area under the plasma concentration time curve, which was calculated using WinNonlin Professional version 4.1 (Pharsight Corporation, Mountain View, CA).[20]

Three weeks after the start of the experiment, all animals received methylprednisolone intramuscularly (20 mg/kg),[14] and were sacrificed at 6 weeks after the start of the experiments. Bilateral femurs were harvested from each animal and served to prepare for histological sections to detect osteonecrosis in the proximal femurs, where the bone marrow necrosis is predominantly noted in the experimental model used in this study.

Preparation of Histological Sections and Detection of Osteonecrosis

The proximal femurs harvested from animals were fixed in 10% buffered formalin and decalcified in 14% EDTA (pH 8). The decalcified femurs were dehydrated in gradient ethanol solutions and embedded in paraffin. The right femurs were cut in coronal plain and a section of mid-coronal portion was analyzed histologically to identify bone or bone marrow necrosis. The left femurs were sectioned vertically to the femoral axis, and the hematoxylin/eosin–stained sections from the femur just distal to the lesser trochanter were analyzed for presence of bone (marrow) necrosis and measurement of percentage necrosis area to the total bone marrow area.

The diagnosis of osteonecrosis was made in blind fashion by three independent authors (TM, KI, and YK). Bone and marrow necrosis was determined based on the diffuse presence of empty lacunae or pyknotic nuclei of osteocytes within the bone trabeculae, accompanied by surrounding bone marrow cell necrosis (Fig. 1).[14,21] The percentage necrotic area in each respective section was measured using a computerized image analyzing system (Nippon Poladigital Co., Tokyo, Japan; Fig. 2).

Based on the histological methods, the incidence of bone or marrow death lesions in each respective group and average percentage necrotic area to total bone marrow area were calculated in the sections with bone or marrow necrosis from the three groups.

Statistical Analysis

The midazolam clearance in each group was analyzed using the unpaired t-test. The incidence of bone necrosis

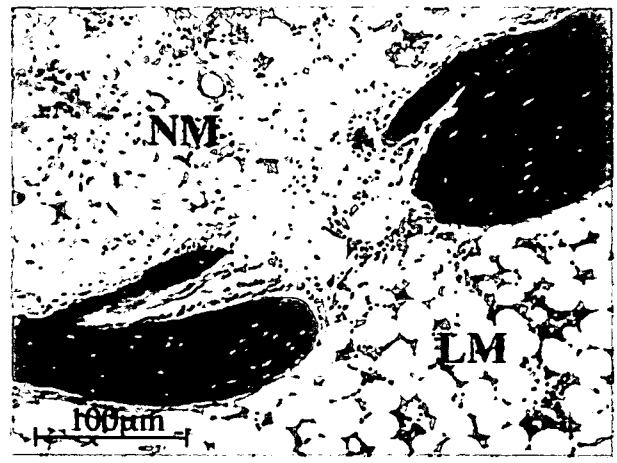

Figure 1. Osteonecrotic lesions in a rabbit model of steroid-induced osteonecrosis. Accumulation of bone marrow cell debris was observed in the necrotic bone marrow (NM). Slight appositional bone formation was noted between NM and living bone marrow (LM). Hematoxylin and eosin stain; original magnification, ×40.

DOI 10.1002/jor

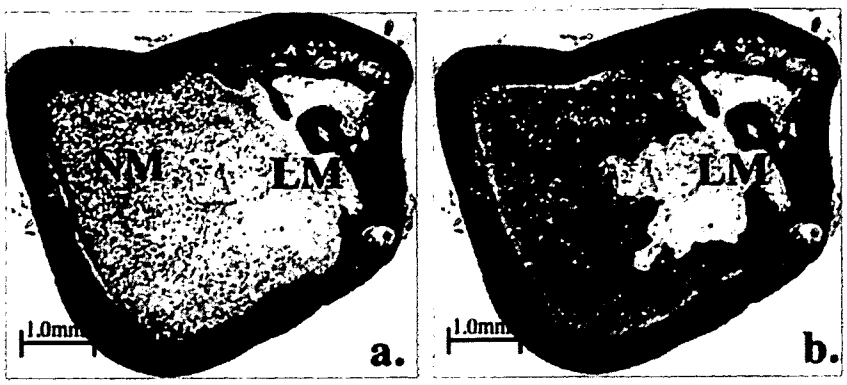

Figure 2. Histological sections at vertical one-third-proximal femora in osteonecrosis-positive rabbits. Lesions were predominantly observed in this level. Percentage area of necrosis was calculated using the following equation: percent area of necrosis (%) = NM/(LM + NM) × 100. NM, necrotic marrow; LM, living marrow. Hematoxylin and eosin stain; original magnification, ×12.5.

in the proximal femur in each respective group was compared using the chi-square test or Fisher's exact probability test. Comparison of percentage necrotic area among the three groups (mean ± SD) was done using one-way analysis of variance (ANOVA). All analyses were performed with SAS statistical software (ver. 9.1, SAS Institute, Cary, NC). Differences of $p < 0.05$ were considered statistically significant.

RESULTS

Midazolam Clearance

No significant difference in body weight among the three groups was noted over the experimental period. There were no significant differences in midazolam clearance between groups P and I at baseline. Compared with baseline, midazolam clearance was significantly increased and decreased after treatment in groups P and I ($p < 0.0005$ and < 0.002, respectively; Fig. 3).

Incidences of Steroid-Induced Osteonecrosis and Percentage Osteonecrosis Area on Histological Section

On histological analyses, bone necrosis was observed in 5 of 15 samples in group P (33%), 15 of 15 samples in group I (100%), and 25 of 30 samples in group C (83%). The incidence of osteonecrosis in group P was significantly lower than that in group I and group C ($p < 0.0001$, $p < 0.001$; Fig. 4). The incidence in group I tended to be slightly higher than that in group C with no statistically significant difference ($p < 0.1$). The mean percentage area of necrosis in whole marrow area on histological cross sections from osteonecrosis-positive rabbits from each group was significantly smaller in group P (8.2 ± 5.9%) than in group C (51.5 ± 30.7%) and group I (69.8 ± 20.8%; $p < 0.005$ for both; Fig. 5). The difference between group C and group I was not significant, although apt to be higher in group C than in group I ($p < 0.1$).

DISCUSSION

In the present study, an increase of CYP3A activity by phenobarbital, as shown by an increased midazolam clearance, significantly reduced the

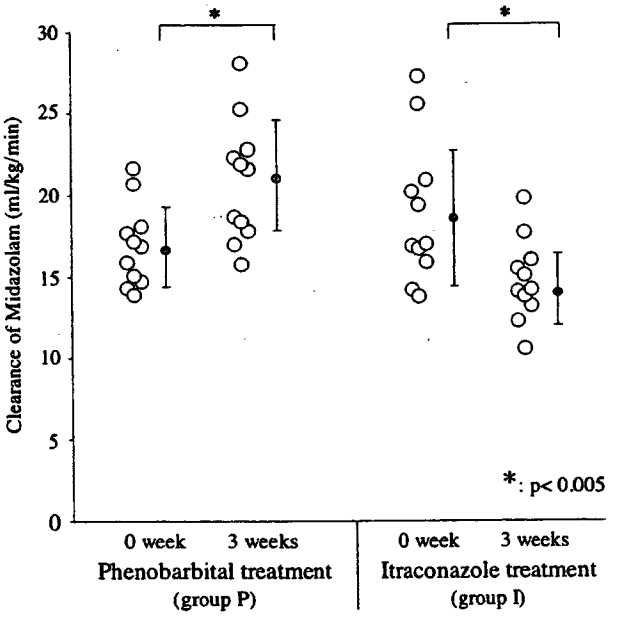

Figure 3. Distribution profiles of midazolam clearance in group P and group I at 0 weeks (baseline) and 3 weeks after the start of treatment. Midazolam clearance is shown as individual values (○) and mean ± SD (● and whiskers). The distribution profile for midazolam clearance in group P at 3 weeks shifted to a significantly higher range compared with that at 0 weeks ($p < 0.0005$), whereas the distribution profile in group I at 3 weeks revealed a significantly lower range of values compared with that at 0 weeks ($p < 0.005$). No significant differences in the distribution profile were seen between group P at 0 weeks and group I at 0 week.

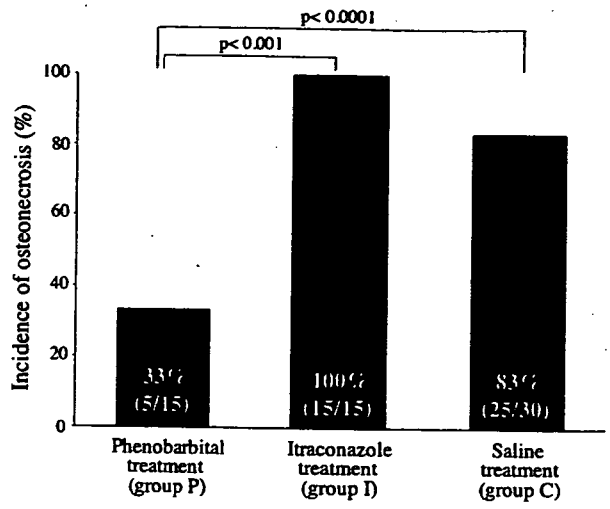

Figure 4. The incidence of osteonecrosis in the three groups. Phenobarbital-treated group (group P) had a significantly lower incidence of osteonecrosis (33%) than control group 83%) and itraconazole-treated group (group I; 100%; ($p < 0.001$, $p < 0.0001$). No significant difference was noted between group I and group C ($p < 0.1$).

incidence of steroid-induced osteonecrosis. This might result from exposure of the femur to lower methylpredonisolone concentration for shorter duration of time by enhanced metabolism by increased CYP3A activity in the liver. Although itraconazole significantly decreased midazolam clearance and the incidence of osteonecrosis was elevated compared with control group, it was not statistically significant. This might result from the relatively high incidence of osteonecrosis in control group (83%). Viewed together, hepatic CYP3A activity plays an important role for the development of steroid-induced osteonecrosis, although the exact mechanism to damage the bony circulation by the high level and prolonged exposure to the exogenous corticosteroid remain to be studied.

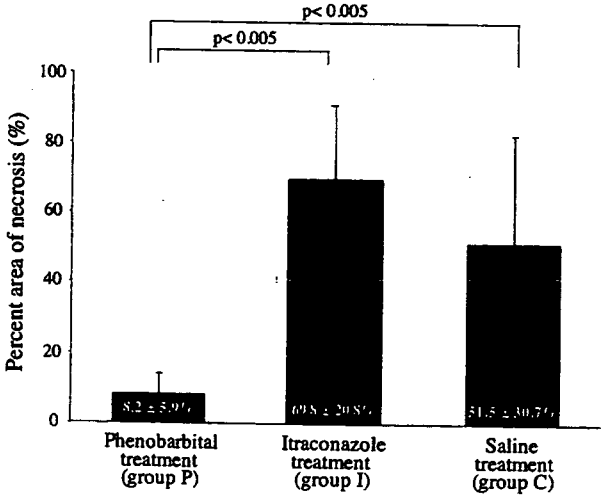

Figure 5. Percentage area of necrosis in the three groups. Phenobarbital-treated group (group P; 8.2 ± 5.9%) had a significantly lower ratio than control group (group C; 51.5 ± 30.7%) and itraconazole-treated group (group I; 69.8 ± 20.8%; $p < 0.005$, $p < 0.005$). No significant difference was noted between group I and group C ($p < 0.1$).

Steroid-induced osteonecrosis model was established by Yamamoto[14] and has been utilized in previous studies.[15–19] In this rabbit model, the steroid-induced bone and marrow necrotic lesions are distributed widely in the skeleton, in sharp contrast with typical ONFH with bone or marrow necrotic lesions limited predominantly in proximomedial part of the femur. In a strict sense, therefore, animal model used in the present study might not be proper as a model of ONFH. However, because osteonecrosis occurs with high incidence (43%–72%) after a single intramuscular injection of high-dose methylpredonizone,[14,18,21] this model might be appropriate for the study of the pathomechanism of steroid-induced bone necrosis. In the present study, the proximomedial parts of the femurs were examined histologically to calculate the incidence and size of bone necrotic lesions caused by steroid treatment with or without modulation of CYP3A activity.

The results are in accordance with previous clinical observations that occurrence of the ONFH associates with maximal daily dose of corticosteroid rather than total dose over the course of treatment,[3,22] indicating exposure of bone to high level of corticosteroids might be a possible risk factor for developing ONFH. Therefore, ONFH, as well as steroid-induced osteonecrosis in other parts of the skeleton, might be caused by excessive or toxic effects of exogenous corticosteroid. The results from the present study also explain our previous clinical observation[11] that the steroid-induced ONFH patients accumulated in population with lower CYP3A activity among general population. Lower CYP3A activity in patients receiving conventional doses of steroids might lead to greater exposure and susceptibility to developing ONFH. These results might provide with possible approach to avoid the ONFH by adjusting the maximal daily dose of corticosteroids depending on the CYP3A activity of the individual patient. For this purpose, more simple and convenient method to measure the CYP3A level in individual patient prior to corticosteroid therapy will be essential. Development of such a method and its validity to avoid the ONFH is under consideration.

In conclusion, the rate of occurrence of steroid-induced osteonecrosis in rabbits with higher hepatic

DOI 10.1002/jor

CYP3A levels, as estimated by midazolam clearance, was significantly lower than in control rabbits. It may be possible to reduce the risk of osteonecrosis by adjusting the dose of corticosteroids to match the metabolic capacity of CYP3A in individual patients.

ACKNOWLEDGMENTS

This study was supported by the Ministry of Education, Culture, Sports, Science, and Technology of Japan (grant-in-aid no.17591590), Takeda science foundation, the Osaka Medical Research Foundation for Incurable Diseases, and the Japanese Investigation Committee under the auspices of the Ministry of Health and Welfare.

REFERENCES

1. Mont MA, Hungerford DS. 1995. Non-traumatic avascular necrosis of the femoral head. J Bone Joint Surg [Am] 77: 459–474.
2. Hirota Y, Hotokebuchi T, Sugioka Y. 1993. Association of alcohol intake, cigarette smoking, and occupational status with the risk of idiopathic osteonecrosis of the femoral head. Am J Epidemiol 137:530–538.
3. Zizic TM, Marcoux C, Hungerford DS, et al. 1985. Corticosteroid therapy associated with ischemic necrosis of bone in systemic lupus erythematosus. Am J Med 79:596–604.
4. Kalla AA, Learmonth ID, Klemp P. 1986. Early treatment of avascular necrosis in systemic lupus erythematosus. Ann Rheum Dis 45:649–652.
5. Varis T, Kivisto KT, Backman JT, et al. 2000. The cytochrome P450 3A4 inhibitor itraconazole markedly increases the plasma concentrations of dexamethasone and enhances its adrenal-suppressant effect. Clin Pharmacol Ther 68:487–494.
6. Varis T, Kivisto KT, Neuvonen PJ. 2000. The effect of itraconazole on the pharmacokinetics and pharmacodynamics of oral prednisolone. Eur J Clin Pharmacol 56: 57–60.
7. Varis T, Kaukonen KM, Kivisto KT, et al. 1998. Plasma concentrations and effects of oral methylprednisolone are considerably increased by itraconazole. Clin Pharmacol Ther 64:363–368.
8. Schellens JH, Soons PA, Breimer DD. 1988. Lack of bimodality in nifedipine plasma kinetics in a large population of healthy subjects. Biochem Pharmacol 37: 2507–2510.
9. Lin YS, Lockwood GF, Graham MA, et al. 2001. In-vivo phenotyping for CYP3A by a single-point determination of midazolam plasma concentration. Pharmacogenetics 11: 781–791.
10. Thummel KE, Shen DD, Podoll TD, et al. 1994. Use of midazolam as a human cytochrome P450 3A probe: I. In vitro-in vivo correlations in liver transplant patients. J Pharmacol Exp Ther 271:549–556.
11. Kaneshiro Y, Oda Y, Iwakiri K, et al. 2006. Low hepatic cytochrome P450 3A activity is a risk for corticosteroid-induced osteonecrosis. Clin Pharmacol Ther 80:396–402.
12. Jones CR, Guengerich FP, Rice JM, et al. 1992. Induction of various cytochromes CYP2B, CYP2C and CYP3A by phenobarbitone in non-human primates. Pharmacogenetics 2:160–172.
13. Venkatakrishnan K, von Moltke LL, Greenblatt DJ. 2000. Effects of the antifungal agents on oxidative drug metabolism: clinical relevance. Clin Pharmacokinet 38:111–180.
14. Yamamoto T, Irisa T, Sugioka Y, et al. 1997. Effects of pulse methylprednisolone on bone and marrow tissues: corticosteroid-induced osteonecrosis in rabbits. Arthritis Rheum 40:2055–2064.
15. Kabata T, Kubo T, Matsumoto T, et al. 2000. Apoptotic cell death in steroid induced osteonecrosis: an experimental study in rabbits. J Rheumatol 27:2166–2171.
16. Miyanishi K, Yamamoto T, Irisa T, et al. 2001. A high low-density lipoprotein cholesterol to high-density lipoprotein cholesterol ratio as a potential risk factor for corticosteroid-induced osteonecrosis in rabbits. Rheumatology (Oxford) 40:196–201.
17. Ichiseki T, Matsumoto T, Nishino M, et al. 2004. Oxidative stress and vascular permeability in steroid-induced osteonecrosis model. J Orthop Sci 9:509–515.
18. Motomura G, Yamamoto T, Miyanishi K, et al. 2004. Combined effects of an anticoagulant and a lipid-lowering agent on the prevention of steroid-induced osteonecrosis in rabbits. Arthritis Rheum 50:3387–3391.
19. Miyanishi K, Yamamoto T, Irisa T, et al. 2005. Effects of different corticosteroids on the development of osteonecrosis in rabbits. Rheumatology (Oxford) 44:332–336.
20. Hamaoka N, Oda Y, Hase I, et al. 1999. Propofol decreases the clearance of midazolam by inhibiting CYP3 A4:an in vivo and in vitro study. Clin Pharmacol Ther 66:110–117.
21. Miyanishi K, Yamamoto T, Irisa T, et al. 2002. Bone marrow fat cell enlargement and a rise in intraosseous pressure in steroid-treated rabbits with osteonecrosis. Bone 30:185–190.
22. Weiner ES, Abeles M. 1989. Aseptic necrosis and glucocorticosteroids in systemic lupus erythematosus: a reevaluation. J Rheumatol 16:604–608.